A NON-DESTRUCTIVE TEST METHOD TO ASSESS THE COMPOSITION OF EXISTING FLOATING FLOORS

Albano Neves e Sousa[1(*)]

[1]ICIST, DECivil, Instituto Superior Técnico (IST), Technical University of Lisbon, Lisbon, Portugal
[(*)]*Email:* albano.nsousa@civil.ist.utl.pt

ABSTRACT

As a consequence of the proliferation of low frequency sound sources, the number of complaints on low frequency noise has increased even in recent constructions. In these situations, field measurements then are required for characterisation of vibration and sound transmission through construction elements in order to define adequate rehabilitation strategies. Unfortunately, current sound transmission measurements are not useful to identify the composition of construction elements although this is fundamental for an adequate designing of sound insulation solutions in the scope of rehabilitation. Simple and non-destructive test methods then are required. As the problem described above often is associated to impact sound transmission through floors, which, in many European countries consist of reinforced concrete slabs with floating covers, in this paper, a non-destructive test method for assessing the composition of such floors is proposed. Particularly, the method is useful for field assessment of the dynamic stiffness and loss factor of elastic interlayers used in floating floor systems available in the market. These properties seldom are provided by manufacturers and field measurements on applied systems offer a cheaper alternative to laboratory tests.

Keywords: *Low frequency sound, floating floors, elastic interlayer, dynamic stiffness, loss factor, field test, non-destructive*

RESUMO

Como consequência da proliferação de fontes de som de baixa frequência, o número de queixas sobre ruído de baixa frequência tem aumentado, mesmo em construções recentes. Nestas situações, são necessárias medições de campo para caracterização da transmissão de vibração e ruído através dos elementos de construção de modo a definir estratégias de reabilitação adequadas. Infelizmente, as medições correntes de transmissão sonora não permitem identificar a composição dos elementos de construção, apesar de ser fundamental conhecê-la para um projecto adequado das soluções de isolamento sonoro no âmbito da reabilitação. Métodos de ensaio simples e não destrutivos são então necessários. Como o problema descrito acima está frequentemente associado à transmissão de ruído de percussão através dos pavimentos, os quais, em muitos países europeus são constituídos por lajes de betão armado com revestimentos flutuantes, no presente artigo, é proposto um método de ensaio não destrutivo para avaliar a composição deste tipo de pavimentos. Em particular, o método é útil para avaliações in situ da rigidez dinâmica e do factor de perdas das camadas elásticas utilizadas nos sistemas de pavimento flutante disponíves no mercado. Estas propriedades raramente são fornecidas pelos fabricantes e, portanto, as medições de campo em sistemas já aplicados constituem uma alternativa mais barata aos ensaios de laboratório

1. INTRODUCTION

According to Grimwood (1997) and Berglund *et al.* (1999), the number of complaints on low frequency noise has increased even in recent constructions, thus requiring the definition of adequate methods for characterisation of vibration and sound transmission to be applied to the design of rehabilitation solutions. These methods should be based on non-destructive field tests which should be able not only to quantify vibration and sound transmission but also to identify the properties of the components of construction elements.

Unfortunately, standard methods for measurement of sound transmission, as descry-bed in Parts 4, 5 and 7 of the standard EN ISO 140 (1998), fail at low frequencies and are not useful for identification of the components of construction elements. Thus, simple and non-destructive test methods are required.

If the problem described above is particularised to impact sound transmission through floors, then some simplifications can be introduced as, in many European countries, floors consist of reinforced homogeneous concrete slabs where floating covers might be applied.

Actually, as floor surfaces are visible, it is possible to assess immediately the characteristics of the bottom and top layers of the floor. As the lower surface of the slab is likely to be rendered, one should look for a part of the building where dropped ceilings are used in order to access the concrete slab surface. Then, a Schmidt hammer can be used to assess the compressive strength of concrete and, consequently, the modulus of elasticity. Usually, the slab thickness can be obtained from licensing projects or, if these are not available, from direct measuring of special parts of the building, such as staircases or balconies.

Initial procedures for assessing the characteristics of the top layer (covering) can be similar to those described for the slab and are aimed mainly at determining the type of covering material and its thickness.

As the mass of typical construction materials normally exhibit small variations around average values, the latter can be used for estimates. Thus, the remaining variables to estimate are the dynamic stiffness and loss factor of the elastic interlayer.

The proposed test method for assessing the composition of floating floors then is based on comparison of predictions with measurements of transfer functions between an impact force and the floor velocity at a given point (floor mobility). Transfer functions between the impact force and the sound pressure at a given point in the room below also can be measured as an alternative. Calculation tools are used iteratively until agreement between transfer function measurements and predictions is reached. Experience has shown that if enough information on the base slab is collected then the number of variables can be reduced, thus allowing quick iterative procedures.

The test method was applied in laboratory and field case studies with promising results (Neves e Sousa and Gibbs, 2011).

2. PREDICTION OF VIBRATION FIELDS IN FLOATING FLOOR SYSTEMS

The proposed test method requires the use of complementary calculation tools which are expected to be used by acousticians for design of insulation solutions in the scope of rehabilitation. As sound fields in room volumes lower than 50 to 60 m^3 exhibit a modal behaviour at low frequencies, as well as vibration fields in structural slabs, deterministic methods are required for prediction of room sound pressures or floor accelerations. The finite element method is often used (Maluski and Gibbs, 2000), although analytical methods based on natural mode analysis also are available. In this paper, the latter method is considered for applications to rectangular rooms and floors with classical edge conditions (Neves e Sousa and Gibbs, 2011).

A floating floor system consists of two plates interconnected by elastic and resilient elements. Such plates in effect are two

coupled systems, which may be described by means of two coupled bending-wave equations. Even if the two plates are separated from each other by a very highly elastic interlayer, as for example in the case of a floating screed on a fibre blanket (Fig. 1), the coupling between the two plates may be significant.

Fibre mats of small thickness can be considered as an array of closely spaced independently acting compression springs, as in a massless Winkler foundation (Cremer, 1973). This approximation seems reasonable, in view of the loose structures of such mats.

As indicated by fundamental theory of dynamics applied to the single degree of freedom mass-spring system, for small damping ratios the attenuation of the dynamic response is only effective for frequencies well above the resonant frequency of the system (Metzen, 1996).

Thus, noise control applications require as small values of the dynamic stiffness (s'') as possible, which means that the mats should be as elastic as possible. However, for installation purposes, the mat cannot be too loosely structured. Introduction in the general bending wave equation of plates of the [very small] pressure $s''(\mu_1 - \mu_2)$ that acts on plates 1 and 2 (Fig. 1) due to the elastic interlayer, and restriction to sinusoidal time variations, leads to the coupled bending-wave equations. The inhomogeneous coupled bending-wave equation can be obtained by considering the external forces per unit area $p_1(y, z)$ and $p_2(y, z)$ that act on the plates. For the case of interest here, only the first plate might be subjected to an arbitrarily distributed continuous load applied over the whole surface, *i.e.*, $p_2(y, z) = 0$ and then

$$B_1' \nabla^4 \mu_1(y, z) - \omega^2 m_1'' \mu_1(y, z) + s'' [\mu_1(y, z) - \mu_2(y, z)] = p_1(y, z); \quad (1.a)$$

$$B_2' \nabla^4 \mu_2(y, z) - \omega^2 m_2'' \mu_2(y, z) + s'' [\mu_2(y, z) - \mu_1(y, z)] = 0; \quad (1.b)$$

where: B_1' and B_2' (Nm) are the flexural stiffnesses of plates 1 and 2, respectively; m_1'' and m_2''(kg/m^2) are the masses per unit area of plates 1 and 2, respectively; and ω (s^{-1}) is the angular frequency.

The solutions of this set of equations correspond to the amplitude of the steady state response of the elastically connected double-plate system and are given by Fourier's expansions depending on the mode shape functions $\varphi_{m_1 n_1}(y, z)$ that satisfy the homogeneous coupled bending-wave equations. The displacement field of the base floor then is given by

$$\mu_2(y, z) = \sum_{m_1 n_1 = 1}^{\infty} [\mu_{2,m_1 n_1}(y, z)] = \sum_{m_1 n_1 = 1}^{\infty} [A_{2,m_1 n_1} \varphi_{m_1 n_1}(y, z)] \quad (2)$$

For a plate of dimensions $b \times c$, the factors $A_{2,m_1 n_1}$ are given by

$$A_{2,m_1 n_1} = \frac{4 \omega_{20}^2 \int_0^b \int_0^c p_1(y, z) \varphi_{m_1 n_1}(y, z) \, dy \, dz}{bc \, m_1'' \left(\omega_{I,m_1 n_1}^2 - \omega^2\right)\left(\omega_{II,m_1 n_1}^2 - \omega^2\right)}, \quad (3)$$

where $\omega_{20} = \sqrt{s''/m_2''}$ is the natural frequency corresponding to vertical vibration of plate 2 for the interlayer acting as a spring with

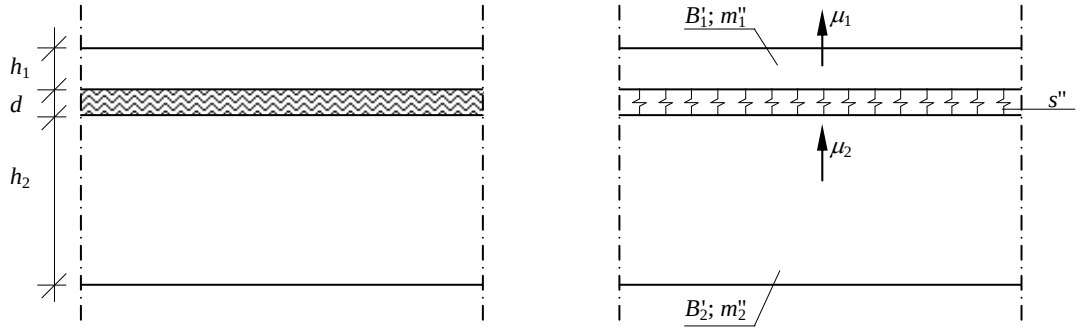

Fig. 1 Schematic representation of floating floor on primary floor structure.

the other plate fixed. According to Cremer (1973) and Oniszczuk (2000), the flexural natural frequencies of the coupled plate, $\omega^2_{\mathrm{I},m_1n_1}$ and $\omega^2_{\mathrm{II},m_1n_1}$, in the denominator of eq. (3) are given by

$$\omega^2_{\mathrm{I},m_1n_1} = \frac{1}{2}\left[\omega^2_{11,m_1n_1} + \omega^2_{22,m_1n_1} \pm \sqrt{\left(\omega^2_{11,m_1n_1} - \omega^2_{22,m_1n_1}\right)^2 + 4\,\omega^4_{120}}\right], \quad (4)$$

where:

$$\omega^2_{11,m_1n_1} = \omega^2_{1,m_1n_1} + \omega^2_{10};$$

$$\omega^2_{22,m_1n_1} = \omega^2_{2,m_1n_1} + \omega^2_{20};$$

$$\omega^4_{120} = \omega^2_{10}\,\omega^2_{20}.$$

Again, $\omega_{10} = \sqrt{s''/m_1''}$. The natural frequencies ω_{1,m_1n_1} and ω_{2,m_1n_1} correspond to the flexural behaviour of the uncoupled plates 1 and 2, respectively.

In the following, eq. (2) will be particularised for two cases, both pertaining to simply supported base floors and sinusoidal point impact forces applied at (y_0, z_0) with amplitude F. The first case corresponds to the simply supported floating floor. For this case, there is an exact solution for the problem. However, floating floors are usually completely free at the edges and therefore another model is required.

The vibration fields of plates 1 and 2 have been described in terms of the displacement. However, in order to obtain the driving-point mobility of the base floor, the vibration field should be written in terms of the transverse velocity by

$$v_{x,2}(y, z) = \mathrm{j}\,\omega\,\mu_2(y, z) = \mathrm{j}\,\frac{4\omega F}{m_1'' bc}\sum_{m_1n_1=1}^{\infty}\left[\frac{\omega^2_{20}\,\varphi_{m_1n_1}(y_0, z_0)\,\varphi_{m_1n_1}(y, z)}{\left(\omega^2_{1,m_1n_1} - \omega^2\right)\left(\omega^2_{\mathrm{II},m_1n_1} - \omega^2\right)}\right], \quad (5)$$

where the mode shape functions that satisfy the homogeneous bending-wave equation for simply supported plates are given by

$$\varphi_{m_1n_1}(y, z) = \sin\left(\frac{m_1\,\pi\,y}{b}\right)\sin\left(\frac{n_1\,\pi\,z}{c}\right). \quad (6)$$

This expression for the amplitude of the steady state forced velocity response of the undamped plate was also derived by Oniszczuk (2004) as part of a general solution containing also the free vibration produced by the application of the exciting loads. In order to include the effect of damping, the denominator of the sum in expression (5) must be substituted by

$$\left(\omega^2_{\mathrm{I},m_1n_1} - \omega^2\right)\left(\omega^2_{\mathrm{II},m_1n_1} - \omega^2\right) = \left[\omega^2_{1,m_1n_1}(1 + \mathrm{j}\,\eta_1) + \omega^2_{10}(1 + \mathrm{j}\,\eta_0) - \omega^2\right] \times \cdots$$

$$\cdots \times \left[\omega^2_{2,m_1n_1}(1 + \mathrm{j}\,\eta_2) + \omega^2_{20}(1 + \mathrm{j}\,\eta_0) - \omega^2\right] - \omega^4_{120}(1 + \mathrm{j}\,\eta_0)^2, \quad (7)$$

where: η_0 is the loss factor of the elastic interlayer; η_1 and η_2 are the loss factors of plates 1 and 2, respectively. The eigenfrequencies ω_{1,m_1n_1} and ω_{2,m_1n_1} are given, for each plate, by

$$\omega_{m_1n_1} = \sqrt{\frac{B'}{m''}}\left[\left(\frac{m_1\,\pi}{b}\right)^2 + \left(\frac{n_1\,\pi}{c}\right)^2\right]. \quad (8)$$

In the case of the free floating floor, the mode shape functions $\varphi_{m_1}(y)$ that satisfy the homogeneous bending-wave equation for fictitious beams free at $y = 0$ and $y = b$ are given by Warburton (1954) and Leissa (1993). Considering that the spatial distribution of the displacements corresponding to each floor mode must be roughly the same in both plates composing the floor (Cremer, 1973) and that the mode shape functions of free floating covers are not applicable to the simply supported base floor, new mode shape functions would have to be found. However, since only the vibration field of the simply supported base floor has to be assessed, the mode shape functions are assumed to be those given by eq. (6), thus satisfying the homogenous bending-wave equation for uncoupled simply supported plates.

The point mobility of the base plate then is given by equations (5) and (7), where the eigenfrequencies ω_{1,m_1n_1} of the floating floor are now given by

$$\omega^2_{m_1n_1} = \frac{B'}{m''}\pi^4\left\{\left(\frac{K_{1,m_1}}{b}\right)^4 + \frac{2\left[\nu K_{2,m_1} K_{2,n_1} + (1-\nu) K_{3,m_1} K_{3,n_1}\right]}{b^2c^2} + \left(\frac{K_{1,n_1}}{c}\right)^4\right\}, \quad (9)$$

with constants K_{1,m_1}, K_{1,n_1}, K_{2,m_1}, K_{2,n_1}, K_{3,m_1} and K_{3,n_1} corrected in order to take into account the fact that floor modes $(m_1 < 2, n_1)$ and $(m_1, n_1 < 2)$ in the free floating floor have no correspondence in

the simply supported base floor. Constants K_{1,m_1}, K_{2,m_1} and K_{3,m_1} then are given by

$$K_{1,m_1} = \left\{ \begin{matrix} 1.506 & \text{for} & m_1 = 1 \\ m_1 + \frac{1}{2} & \text{for} & m_1 \geq 2 \end{matrix} \right\}; \tag{10.a}$$

$$K_{2,m_1} = \left\{ \begin{matrix} 1.248 & & \text{for} \quad m_1 = 1 \\ \left(m_1 + \frac{1}{2}\right)^2 \left[1 - \frac{2}{\pi\left(m_1 + \frac{1}{2}\right)}\right] & & \text{for} \quad m_1 \geq 2 \end{matrix} \right\}; \tag{10.b}$$

$$K_{3,m_1} = \left\{ \begin{matrix} 5.017 & & \text{for} \quad m_1 = 1 \\ \left(m_1 + \frac{1}{2}\right)^2 \left[1 + \frac{6}{\pi\left(m_1 + \frac{1}{2}\right)}\right] & & \text{for} \quad m_1 \geq 2 \end{matrix} \right\}. \tag{10.c}$$

Constants K_{1,n_1}, K_{2,n_1} and K_{3,n_1} are obtained by replacing m_1 by n_1 in the above expressions.

The prediction method described by equations (5) and (7) is easy to implement and calculations are fast. The method was validated by laboratory and field tests.

3. LABORATORY VALIDATION TESTS

The driving-point mobility of the top floor of a laboratory test room was measured for five different types of floating floors in order to validate the models proposed. The base floor is a 105 mm thick concrete plate whose top surface had been smoothed by adding a hard epoxy mortar layer. The bottom surface is covered by a 10 mm layer of common mortar and a 5 mm layer of plaster. The floor area is 1.82 m × 2.87 m = 5.23 m^2.

The floating floors to be tested had to satisfy two conditions, which were: to be reusable and non permanent in order to allow repeating experiments at a later time; to be light enough to be transported to the test floor. Medium density fibreboards (MDF) fulfil both requirements and therefore 18 and 40 mm sheets were used for the top plate of the tested floating floors.

The 18 mm sheet was tested on two different resilient layers: a) a 15 mm thick recycled low-resonance acoustic chip (LRAC) foam layer (Fig. 2); and b) a 25 mm rockwool layer. The point mobility obtained with case a) was compared with that obtained with case c), which is a floating floor composed by 18 mm *VIROC* tongued and grooved chipboards with bonded 15 mm thick LRAC foam layers. The 40 mm MDF sheet also was tested on: d) a 15 mm thick LRAC foam layer; and e) a 25 mm rockwool layer.

The small wooden "bridge" with white straps that can be seen in Fig. 2 was used to avoid inserting vibrations from the human body on the floor during manual hammer impacts.

The MDF sheets, with dimensions of 1.20 m × 2.40 m = 2.88 m^2 did not cover the whole surface of the floor (Fig. 2). It was assumed that, for impacts away from the edges, the behaviour of the floor would be similar to that shown by a floating floor covering the whole area.

For each tested floating floor, the driving-point mobility was measured in three different points, located along the diagonal shown in Fig. 2, for the same three different points of impact, which gave nine measured point mobilities.

Measurements of the driving-point mobility were made with a Brüel & Kjær's dual channel real-time frequency analyser type 2144. Averages were taken from 64 hits for each measurement. One channel recorded the force applied by a calibrated hammer with a B&K's force transducer type 8200. The second channel recorded the acceleration measured on the excited floor by a B&K's accelerometer type 4381. Both signals were amplified by a B&K's NEXUS conditioning power amplifier type 2192.

The mass m_0 of the hammer does not affect the measured mobility if its impedance $j\omega m_0$ is small compared with the driving-point impedance Z of the plate. This condition is usually satisfied for primary floor structures over the entire frequency range of interest (Cremer, 1973). However, for the lighter floating floor structures, the mass impedance of the hammer becomes significant at frequencies above a limiting frequency given by Z_1/m_0 (in rad/s), where $Z_1 \approx 8\sqrt{B'm_1''}$ is the characteristic driving-point impedance of the uncoupled floating

floor. In the present case, as only low frequencies are of interest, this limitation is less problematic. Illustratively, it can be pointed out that the characteristic driving-point impedance of the tested 18 mm MDF plate is 1068.2 s/kg, which means that any hammer with mass lower than 850 grams, as the one used in this work, can be used for mobility measurements below 200 Hz. Predictions of the driving-point mobility were obtained by equations (5) and (7) after setting the properties of the materials. Considering common densities of the identified materials, the equivalent value ρ_{base} = 2,620 kg/m^3 was adopted for the whole floor. The equivalent modulus of elasticity was assumed as E_{base} = 25.2 GPa, which has been adjusted from impact tests with a Schmidt hammer on the concrete plate. According to the manufacturers, MDF has a density of at least ρ_{MDF} = 730 kg/m^3. For predictions, an average value of the elasticity modulus, E_{MDF} = 2.45 GPa, was used. The Poisson's ratio was assumed as ν = 0.35. In order to compare measured and predicted driving-point mobilities for the five floating floors tested, preliminary tests had to be done to assess the properties of the resilient materials. The standard method for determining the dynamic stiffness of materials used under floating floors is contained in EN 29052 – 1 (1992). Despite this standard does not apply to loadings lower than 0.40 kPa, according to Hall (1997), the method is still useful for determining the dynamic stiffness of the test samples of the resilient layers used for experimental validation of the prediction model derived in the previous section. According to Vér (1974), Pritz (1994 and 1996), Hall (1997), Stewart and Craik (2000), Stewart and Makenzie (2000), and Schiavi *et al.* (2005), at low frequencies, there is no significant increase with frequency in either the dynamic Young's modulus or the loss factor of resilient materials, thus allowing the standard EN 29052 - 1 (1992) to be used to determine experimentally the dynamic stiffness of such materials.

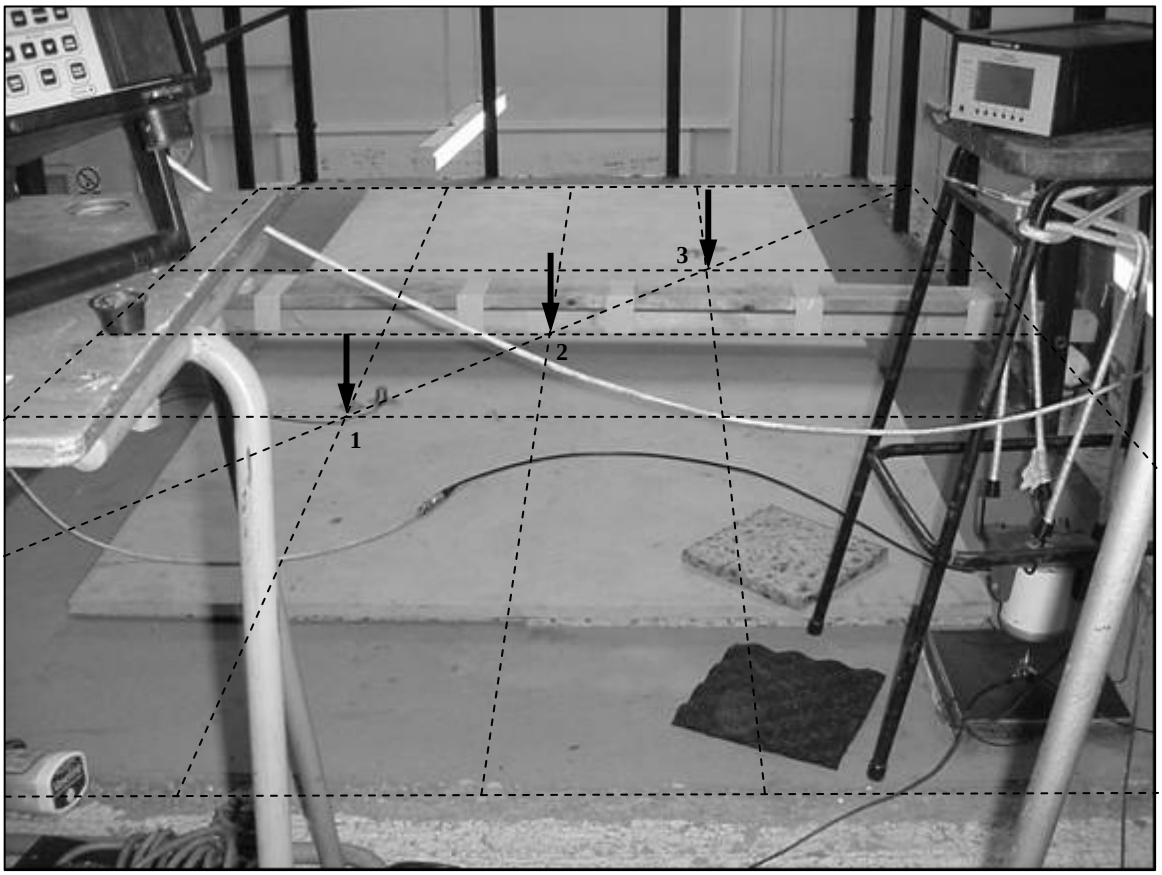

Fig. 2 Tested 18 mm MDF sheet on the 15 mm recycled LRAC foam and points for mobility measurements.

This standard defines dynamic stiffness as the ratio of dynamic force to dynamic displacement. It identifies the fundamental vertical frequency of vibration f_r of a standard mass-spring test system and uses this to calculate the apparent dynamic stiffness s''_{app} of the test specimen per unit area using the relationship

$$f_r = \frac{1}{2\pi}\sqrt{\frac{s''_{app}}{m''_t}} \Rightarrow s''_{app} = m''_t \left(2\pi f_r\right)^2, \qquad (11)$$

where m''_t is the total mass per unit area used during the test. For highly damped systems, the standard EN 29052 - 1 recommends monitoring the input-output phase difference.

In the present study, the measurements were made as illustrated in Fig. 3. A shaker excited a 3 mm thick steel plate with dimensions of 20 cm × 20 cm. The mass of the steel plate was 913.73 grams. The force exerted by the shaker was measured by a B&K's force transducer type 8200. The acceleration was measured on the steel plate by a B&K's accelerometer type 4393 connected to it. Both signals fed into a B&K's dual-channel real time frequency analyser type 2144

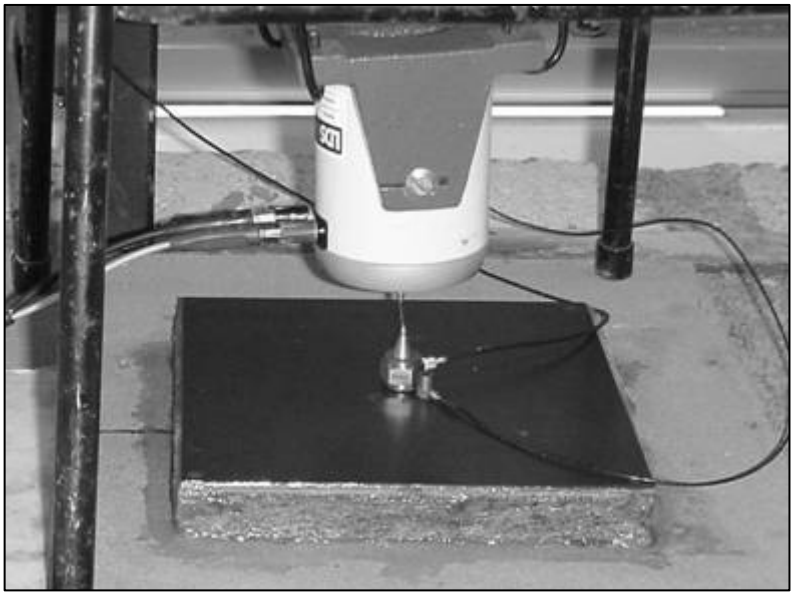

Fig. 3 Set-up for the measurement of dynamic stiffness.

As it has been done by Hall (1997), the plaster of Paris layer between the sample and the load plate which is specified by EN 29052 - 1 (1992) was not used because the surface of the samples was considered smooth enough. The sides of the sample were sealed with a fillet of petroleum jelly to ensure that the air did not move laterally beneath the test specimen. Thus, the effect of the airflow resistivity of the material is indirectly taken into account.

The above described procedure indicated a dynamic stiffness s'' = 12.5 MN/m^3 for the recycled LRAC foam for a resonance frequency of 117.5 Hz, with a loss factor η = 0.38. The measured density of the recycled LRAC foam was 103.0 kg/m^3.

The tests made on the rockwool sample indicated a dynamic stiffness s'' = 8.2 MN/m^3 for a resonance frequency of 95 Hz. Although the measured dynamic stiffness is lower than the minimum dynamic stiffness given in manufacturer's technical tables (11.2 MN/m^3), it is in close agreement with values given by Cremer *et al.* (1973) and Stewart and Makenzie (2000). The measured loss factor was η = 0.43, which seems high. Loss factors given by Cremer *et al.* (1973) and Stewart and Craik (2000) are less than 0.10. The measured density of the rockwool was 158.4 kg/m^3.

The loss factor, considered in mobility predictions, for the simply supported top plate was assumed as given in EN ISO 12354 – 1 (2000). In the case of the

free floating floor, the coupling losses were neglected and thus the loss factor was assumed as constant and equal to $\eta = 0.015$.

Figures 4 and 5 show the magnitude of measured and predicted driving-point mobilities for the base floor alone and for the base floor with the floating floor a), which is composed by the 18 mm MDF sheet resting on a 15 mm layer of LRAC foam. The predicted driving-point mobility of the base plate was given by

$$v_x(y, z) = \mathrm{j}\,\frac{4\,\omega F}{m''\,b\,c}\sum_{m_1,n_1=1}^{\infty}\left[\frac{\varphi_{m_1n_1}(y, z)\,\varphi_{m_1n_1}(y_0, z_0)}{(\omega^2_{m_1n_1} - \omega^2)}\right]. \qquad (12)$$

Mobility measurements are also shown for the base floor with the floating floor c), which is composed by 18 mm VIROC tongued and grooved chipboards bonded to a 15 mm LRAC foam layer. The plotted measured mobilities correspond to the averages of reciprocal and symmetric mobilities. The predicted mobilities were obtained with eq. (5) considering either a simply supported or a free floating floor. The properties of the VIROC tongued and grooved chipboards were assumed equal to those of the 18 mm MDF sheet.

Fig. 4 shows the driving-point mobility at $(y, z) = (b/3, c/3)$ for an impact force applied at the same point. Fig. 5 shows the transfer functions between the impact force applied at $(y_0, z_0) = (b/2, c/2)$ and the transverse velocities at $(y, z) = (b/3, c/3)$ and $(y, z) = (2b/3, 2c/3)$.

Visual inspection of Figures 4 and 5 and of other similar plots shows that the floating floor systems a) and c) have approximately the same properties. For both floating floor systems, the cut-off frequency f_{12}, below which the interlayer acts as if it were infinitely stiff (not compressed), thus yielding approximately the same vibration field in both plates (very small attenuation), is 159 Hz as obtained from

$$f_{12} = \frac{1}{2\pi}\sqrt{s''\left(\frac{1}{m_1''} + \frac{1}{m_2''}\right)}. \qquad (13)$$

Below this frequency, the floor tends to behave as a plate with bending stiffness given by the sum of the bending stiffnesses of the two plates and with mass per unit area also given by the sum of the masses per unit area of the two plates. In the case of floating floors a) and c), this behaviour approaches that of the base floor. However, in the frequency range 100 - 140 Hz, which includes the frequency at which the floor mode (1, 2) occurs, the floating floor still affects the vibration of the base plate and increases the mobility. This effect appears both in measured and predicted point mobilities. The reduction in mobility due to

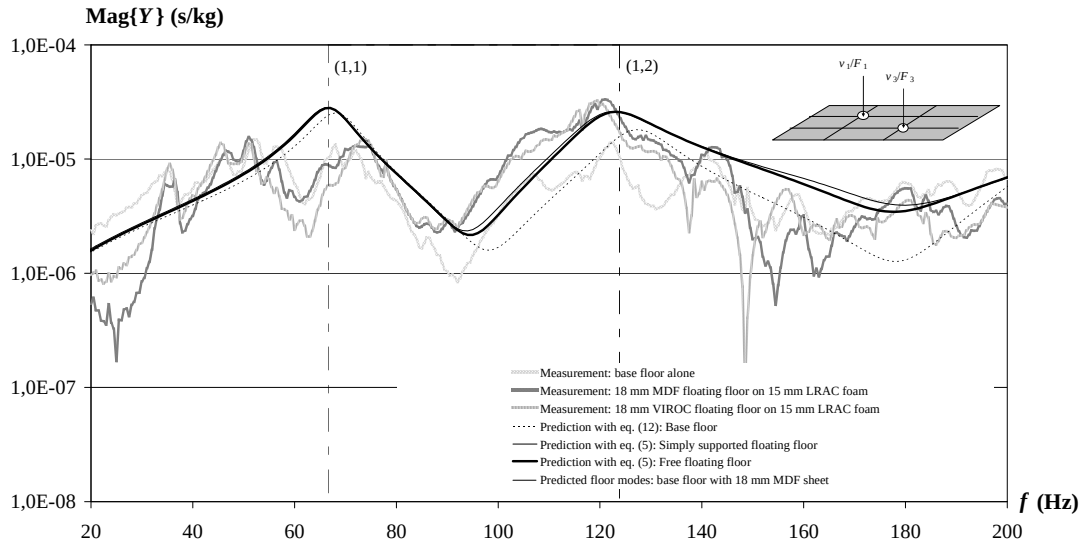

Fig. 4 Measured and predicted point mobilities at $(y, z) = (b/3, c/3)$ for an impact force applied at the same point on the base floor covered with a 15 mm LRAC foam layer topped by: a) an 18 mm MDF sheet; b) 18 mm VIROC tongued and grooved chipboards.

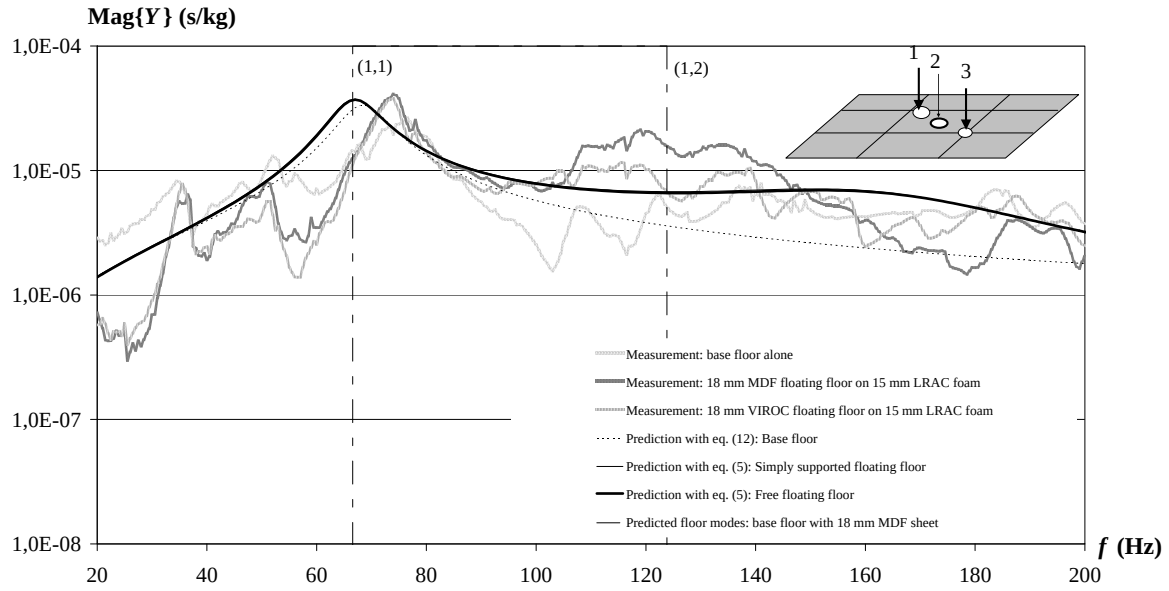

Fig. 5 Measured and predicted transfer functions between $F[(y_0, z_0) = (b/2, c/2)]$ and $v_x[(y, z) = (b/3, c/3)]$ and $v_x[(y, z) = (2b/3, 2c/3)]$ and their reciprocals for the base floor covered with a 15 mm LRAC foam layer topped by: a) an 18 mm MDF sheet; b) 18 mm tongued and grooved chipboards.

floating floors occurs only above f_{12}. This effect is visible in measured mobilities (Figures 4 and 5) above 180 Hz but occurs only above 200 Hz in predicted mobilities

Figures 6 and 7 show the magnitude of the measured and predicted driving-point mobilities for the base floor alone and with the floating floor b), which is composed by the 18 mm MDF sheet resting on a 25 mm rockwool layer. Again, the plotted measured mobilities correspond to the averages of reciprocal and symmetric mobilities. The mobilities shown in Fig. 6 refer to the same points than in Fig. 5. Fig. 7 shows the driving-point mobilities at $(y, z) = (b/2, c/2)$ for an impact force applied in the same point.

For floating floor b), predicted f_{12} is 129 Hz, which means that higher mobilities are expected in the vicinity of f_{12} than with the floating floors based on 15 mm LRAC foam layers. This effect is

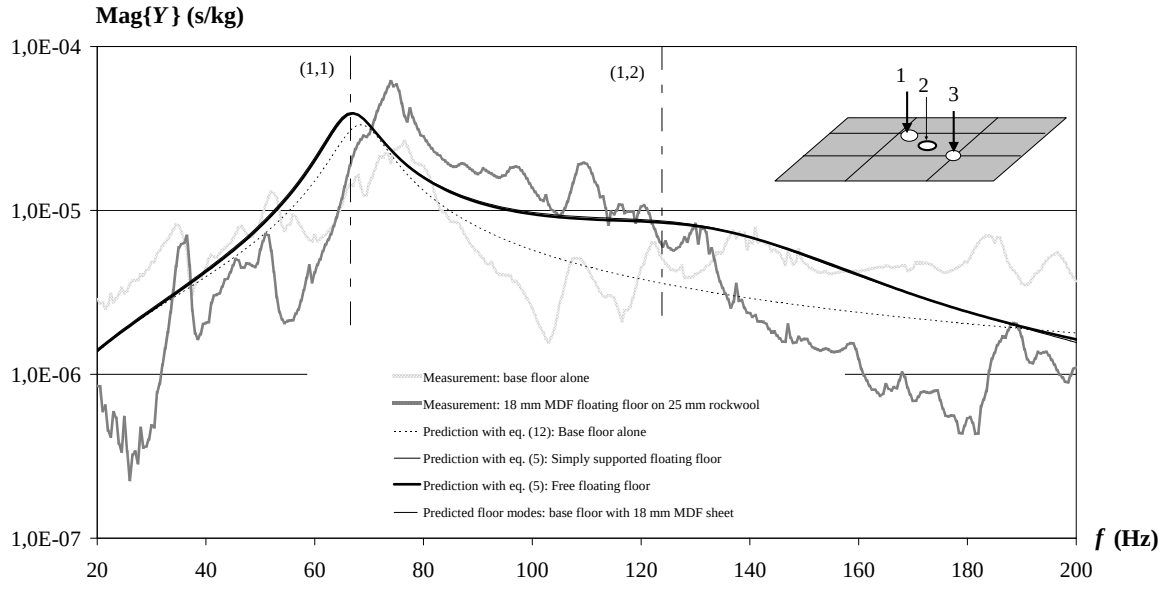

Fig. 6 Measured and predicted transfer functions between $F[(y_0, z_0) = (b/2, c/2)]$ and $v_x[(y, z) = (b/3, c/3)]$ and $v_x[(y, z) = (2b/3, 2c/3)]$ and their reciprocals for the base floor covered with a 25 mm rockwool layer topped by an 18 mm MDF sheet.

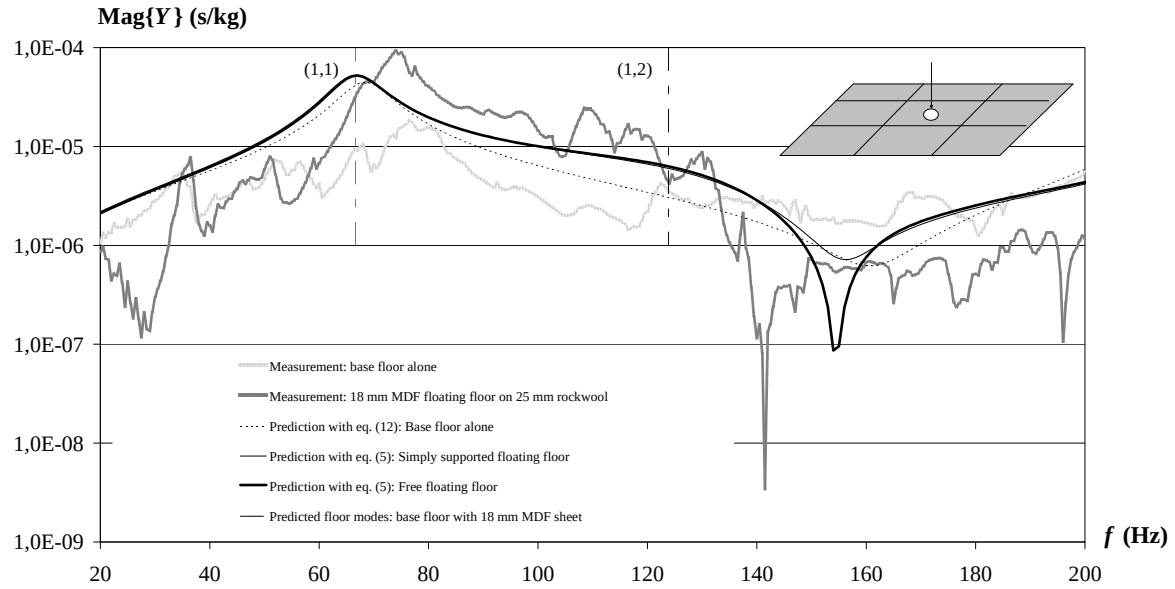

Fig. 7 Point mobility measured and predicted at (y, z) = (b/2, c/2) for an impact force applied at the same point in the base floor covered with a 25 mm rockwool layer topped by an 18 mm MDF sheet.

more evident in Fig. 6. Since f_{12} is lower than in the previously studied floating floors, the improvement in the floor response occurs now clearly for frequencies above 150 Hz, approximately. This effect is now also visible in predicted mobilities but only above 185 Hz.

Figures 4 to 7 show that there are no significant differences between the predicted mobilities obtained for the simply supported and free floating floors. The agreement with experimental values is generally good.

The three floating floors - a), b) and c) - discussed above have frequencies f_{12} relatively high compared with the frequency range studied in this paper. However, the frequencies f_{12} can be decreased by increasing the mass of the floating floors – cases d) and e).

The point mobility measurements were repeated for floating floors d) and e), which are composed by a 40 mm MDF sheet resting on the 15 mm LRAC foam layer and on the 25 mm rockwool layer, respectively.

Figures 8 and 9 show the magnitude of the measured and predicted driving-point mobileties for case d). Again, the plotted measured

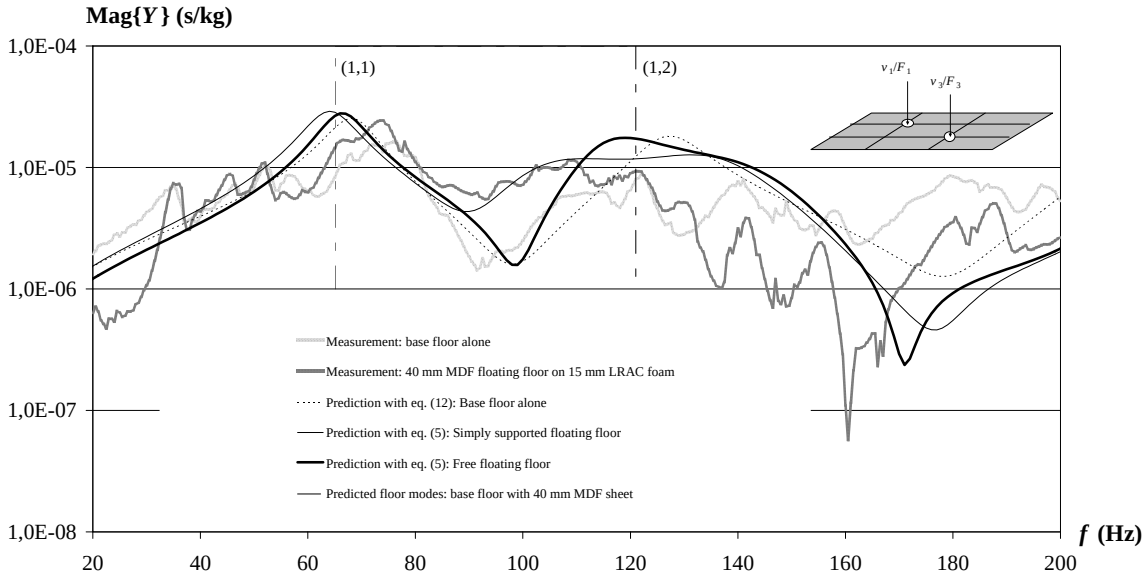

Fig. 8 Measured and predicted point mobilities at (y, z) = (b/3, c/3) for an impact force applied at the same point on the base floor covered with a 15 mm LRAC foam layer topped by a 40 mm MDF sheet.

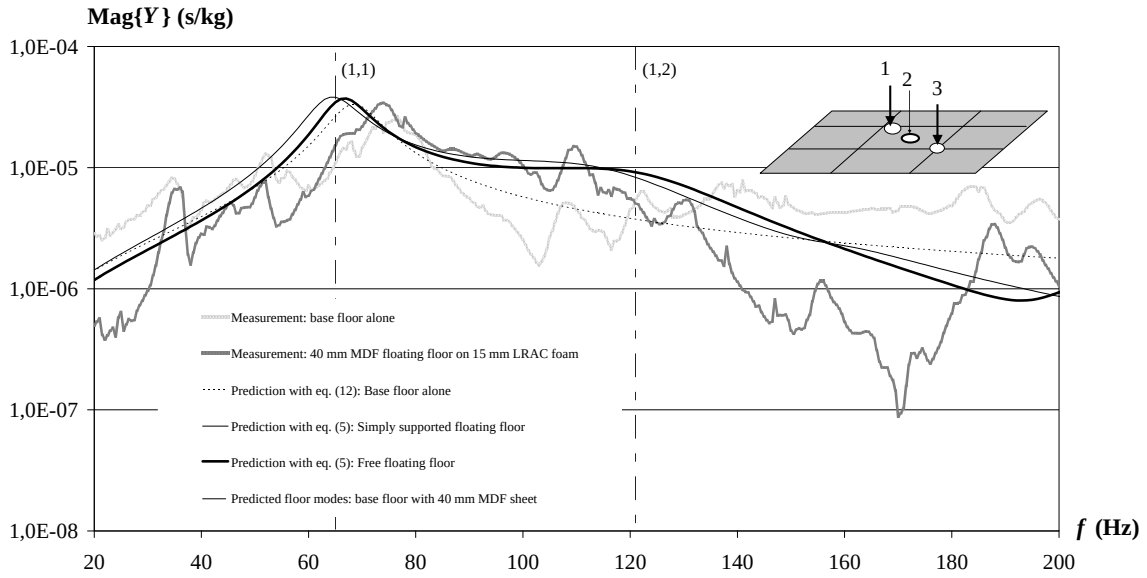

Fig. 9 Measured and predicted transfer functions between $F[(y_0, z_0) = (b/2, c/2)]$ and $v_x[(y, z) = (b/3, c/3)]$ and $v_x[(y, z) = (2b/3, 2c/3)]$ and their reciprocals for the base floor with a 15 mm LRAC foam layer topped by a 40 mm MDF sheet.

mobilities correspond to the averages of reciprocal and symmetric mobilities at the same points than in Figures 4 and 5, respectively. The frequency f_{12} in case d) is 109 Hz and the increase in mobility in that frequency was confirmed by measurement results. The improvement in the floor response is now obvious for frequencies above 130 Hz. Again, the predicted mobilities exhibit the improvement only for frequencies above 165 Hz, approximately.

Although differences between the predicted mobilities obtained for the simply supported and free floating floors are now more easily identified, the predicted mobility curves are still too close to each other and it is difficult to identify which one gives the better approximation to measured mobilities

Finally, Figures 10 and 11 show the magnitude of the measured and predicted driving-point mobilities for case e). The plotted measured and predicted mobilities were obtained in the same conditions described for cases a) to d). The frequency f_{12}

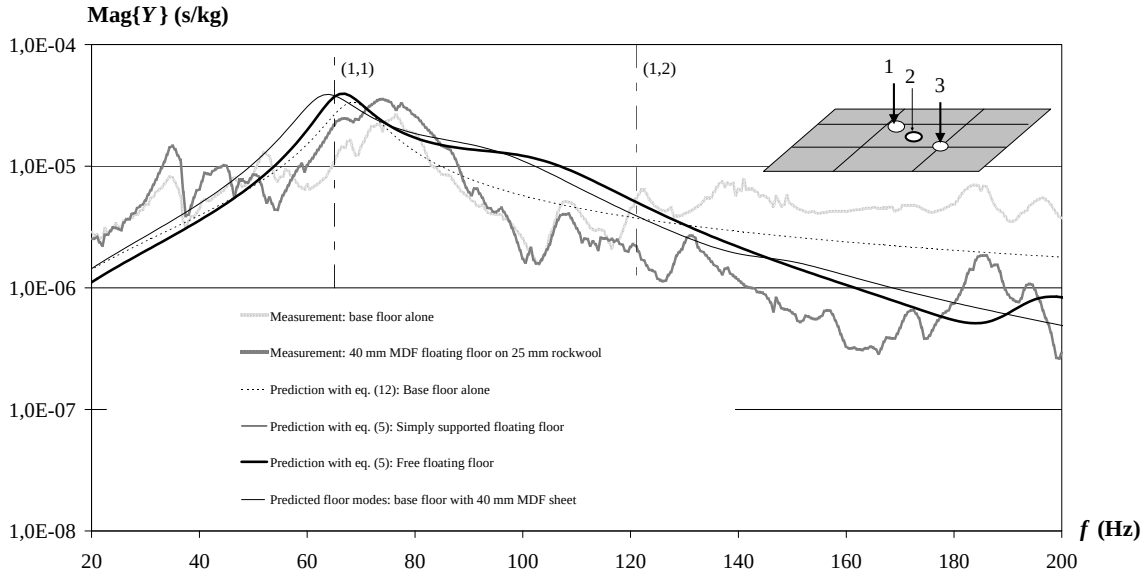

Fig. 10 Measured and predicted transfer functions between $F[(y_0, z_0) = (b/2, c/2)]$ and $v_x[(y, z) = (b/3, c/3)]$ and $v_x[(y, z) = (2b/3, 2c/3)]$ and their reciprocals for the base floor covered with a 25 mm rockwool layer topped by a 40 mm MDF sheet.

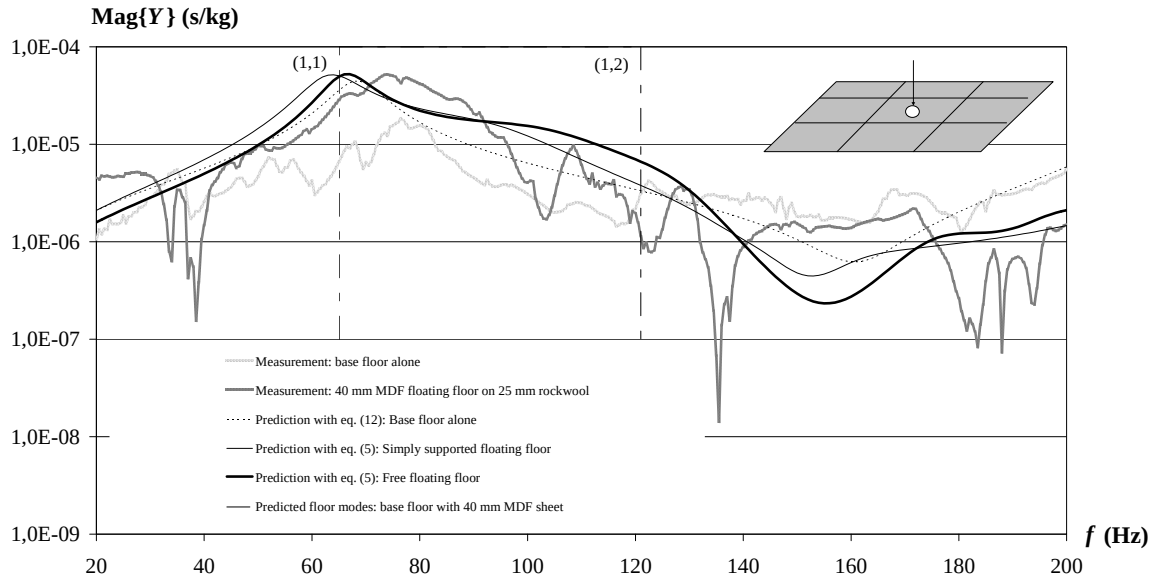

Fig. 11 Point mobility measured and predicted at (y, z) = (b/2, c/2) for an impact force applied at the same point in the base floor covered with a 25 mm rockwool layer topped by a 40 mm MDF sheet.

in case e) is 88 Hz and the increase in mobility in the vicinity of that frequency was again confirmed by measurement results. The improvement inthe floor response is now obvious for frequencies above 120 Hz. Again, the predicted mobilities are improved only for higher frequencies, approximately above 135 Hz. The predicted mobilities are again in good agreement with measured mobilities and therefore the models given by eq. (5) for the driving-point mobility of floors with floating floors are validated.

4. *IN SITU* VALIDATION TESTS

The models were also validated by *in situ* mobility measurements. These measurements were made in a 20 years old multi-storey building, located in Lisbon, with a traditional concrete frame structure. Fortunately, the measurements were made in a duplex apartment, which allowed an accurate estimate of the slab thickness. The following materials were identified: a bottom 5 mm layer of plaster; a 155 mm reinforced concrete slab; a 17 mm layer of mortar; a 5 mm layer of a resilient material; and an 8 mm layer of oak parquet.

The densities of the materials constituting the base plate were assumed as:

$\rho_p = \rho_{plaster} = 1200$ kg/m^3;

$\rho_c = \rho_{concrete} = 2450$ kg/m^3;

$\rho_m = \rho_{mortar} = 2100$ kg/m^3.

The density of an equivalent concrete cross-section with 155 mm of thickness is approximately 2720 kg/m^3. Only the reinforced concrete and mortar layers were considered in the bending stiffness of the base plate. The modulus of elasticity of concrete was estimated from the compressive strength of a C20/25 concrete at an age of 20 years, which is approximately $\sigma_{cm} = 1.45 \times 28 = 40.6$ MPa according to EN 1992-1-1. The corresponding modulus of elasticity is $E_c = 33.4$ GPa. The modulus of elasticity of the mortar layer was initially assumed as $E_m = 13.7$ GPa (Brazão Farinha, 1996) and cracking was not considered, however, predicted driving-point mobilities agreed better with measured values for $E_m = 11$ GPa. The modulus of elasticity for the equivalent concrete cross-section with 155 mm of thickness was found to be 34.3 GPa. The Poisson's ratio for the concrete equivalent cross-section was assumed as $\nu = 0.15$.

The properties of the oak parquet were assumed as $E_{oak} = 2$ GPa and $\rho_{oak} = 750$ kg/m^3. Since there were furniture in the room where the floating floor was installed (Fig. 12), the density was increased in order to take into account the

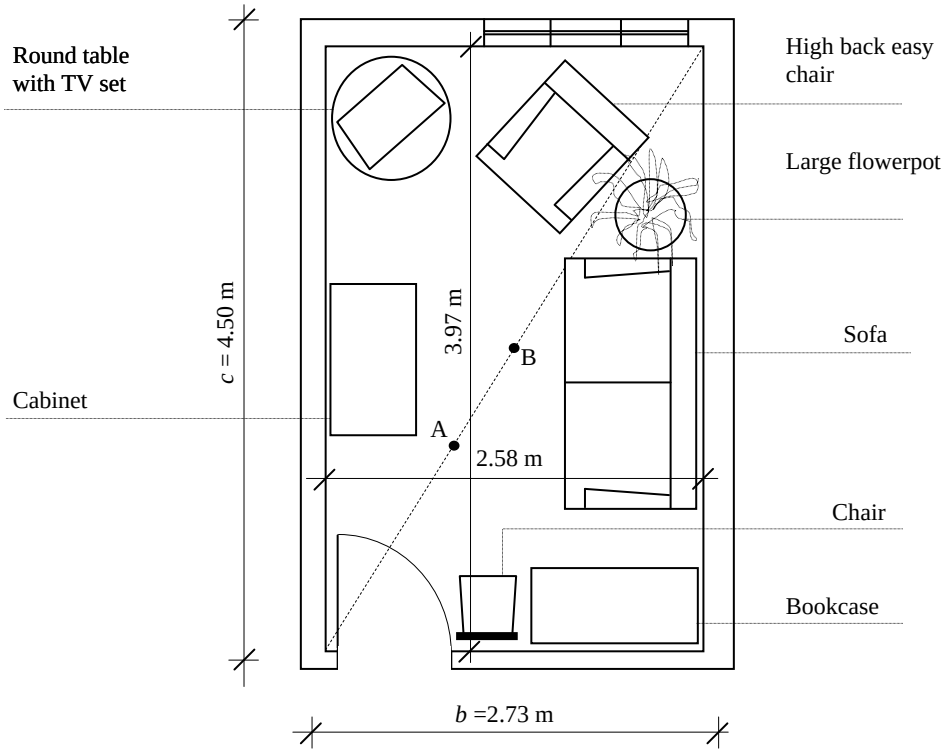

Fig. 12 Furniture on the tested floor.

mass of furniture. Also the mass of the experimenter and of the measurement equipment were considered. The total mass added to the floating floor was assumed as approximately 310 kg, which gave an additional density of 3795 kg/m^3. Thus, the total density of top plate used in mobility predictions was 4545 kg/m^3.

The driving-point mobilities were measured in points A and B (Fig. 12), which correspond to coordinates $(y, z) = (b/3, c/3)$ and $(y, z) = (b/2, c/2)$, respectively.

The measured mobilities are shown in Figures 13 and 14. Fig. 13 shows the driving-point mobility at point A. Fig. 14 shows the transfer function between the impact force applied at A and the

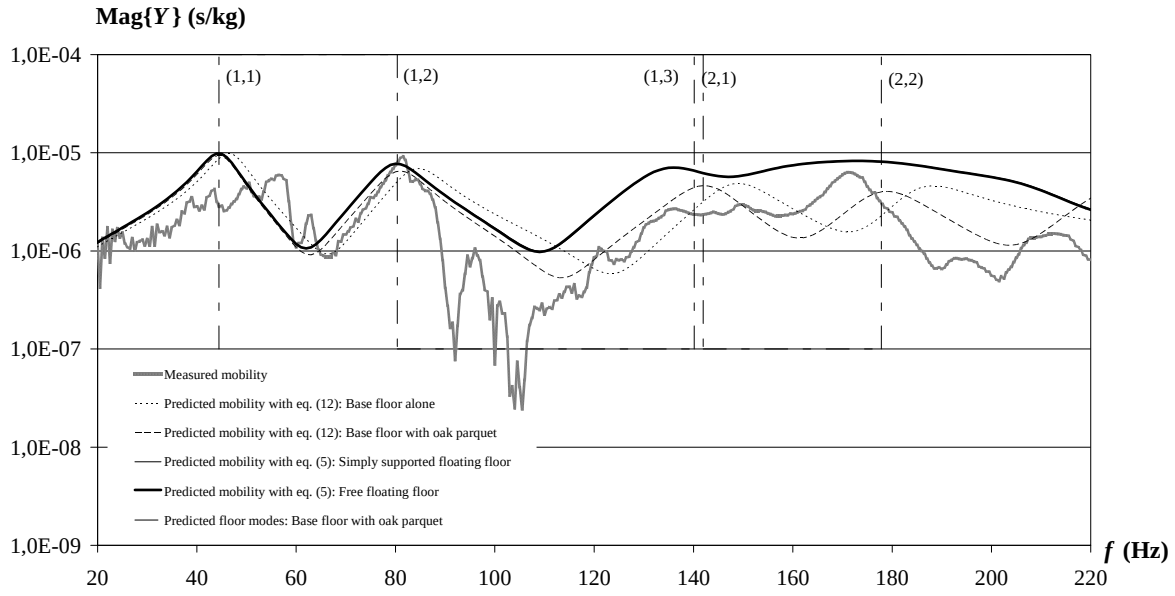

Fig. 13 Measured and predicted point mobilities at $(y, z) = (b/3, c/3)$ for an impact force applied at the same point on the base floor covered with a 5 mm layer of resilient material topped by 8 mm oak parquet.

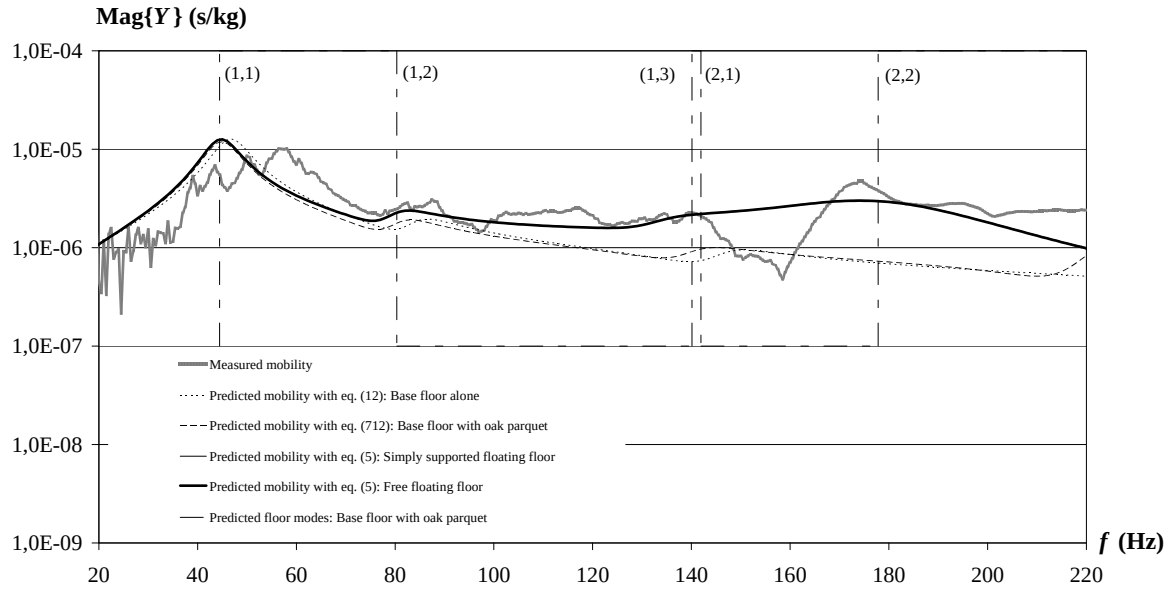

Fig. 14 Measured and predicted transfer functions between $F[(y_0, z_0) = (b/3, c/3)]$ and $v_x[(y, z) = (b/2, c/2)]$ and their reciprocals for the base floor with a 5 mm layer of resilient material topped by 8 mm oak parquet.

transverse velocity at B and also the reciprocal transfer function. The predicted mobilities were obtained with eq. (5) considering either a simply supported or a free floating floor. Predictions of the point mobilities obtained with eq. (12) for the base and top plates, without the resilient layer, are also shown in Figures 13 and 14. Comparison of measured mobilities with predicted values obtained for the base floor with the oak parket, without the resilient layer, shows that the floor mobility is increased around 175 Hz, probably due to the floating floor. Therefore, the initial value of the stiffness of the resilient layer was chosen so that f_{12} should be around 175 Hz.

After a quick iterative process, s'' was adjusted to 41.6 MN/m^3, for which f_{12} became approximately 177 Hz. The loss factor of the resilient layer was adjusted to $\eta = 0.25$. The predicted mobilities obtained with the adjusted values of s'' and η are generally in good agreement with experimental values. Thus, even if the properties of the resilient layer are not known, it is possible to back calculate them using eq. (5).

Similar conclusions are drawn if transfer functions between impact force and sound pressure are considered as shown by Neves e Sousa (2005). In this case, the required predictions of sound pressure fields could be obtained as suggested by Neves e Sousa and Gibbs (2011) based on the work of Kihlman (1967) and Vieira de Melo (2006).

5. CONCLUSION

Models for the driving-point mobility of plates with simply supported and free floating floors have been derived from natural mode analysis. The models apply to homogeneous simply supported base plates of uniform thickness with homogenous floating floors.

Both models were experimentally validated in the laboratory and *in situ*.

Differences between the two models were found to be insignificant in the cases studied.

In all studied cases, the cut-off frequency f_{12} was in the frequency range 20 – 200 Hz, and therefore increases in floor mobility were expected in this frequency range in relation to bare floors.

Although very little information on the dynamic stiffness and loss factor of resilient materials is released by manufacturers (Neves e Sousa, 2005), these properties can be assessed in the field by non-destructive measurements of the floor mobility.

6. REFERENCES

Berglund B, Hassmén P, Job RFS. Sources and effects of low frequency noise. Journal of the Acoustical Society of America, 1999, 5, p. 2985-3002.

Brazão Farinha JS; Correia dos Reis A. Technical tables (in Portuguese; Original title: Tabelas técnicas), Edições Técnicas, Lisbon, Portugal, 1996;

Cremer L, Heckl M, Ungar EE. Structure-borne sound – Structural vibrations and sound radiation at audio frequencies. 2nd edition, Springer-Verlag, Berlin, Germany, 1973.

European Committee for Standardization, EN ISO 140 – 4: Acoustics – Measurement of sound insulation in buildings and of building elements – Part 4: Field measurements of airborne sound insulation between rooms, 1998.

European Committee for Standardization, EN ISO 140 – 5: Acoustics – Measurement of sound insulation in buildings and of building elements – Part 5: Field measurements of airborne sound insulation of façade elements and façades, 1998.

European Committee for Standardization, EN ISO 140 – 7: Acoustics – Measurement of sound insulation in buildings and of building elements – Part 7: Field measurements of impact sound insulation of floors, 1998.

European Committee for Standardization, EN 1992-1-1: Eurocode 2 – Design of concrete structures – Part 1: General rules and rules for buildings, 2004;

European Committee for Standardization, EN ISO 12354 – 1: Building acoustics – Estimation of acoustic performance of buildings form the performance of elements – Part 1: Airborne sound insulation between rooms, 2000;

European Committee for Standardization, EN ISO 29052 – 1. Acoustics – Materials for acoustical applications – Materials used under floating floors in dwellings, 1992.

Grimwood C. Complaints about poor sound insulation between dwellings in England and Wales. Applied Acoustics, 1997, 3/4, p. 211-223.

Hall R. Impact sound insulation of flooring systems with polyurethane foam on concrete floors, Ph. D. Thesis, Sheffield Hallam University, Sheffield, UK, 1997.

Kihlman T. Sound radiation into a rectangular room. Applications to airborne sound transmission in buildings. Acustica, 1967, 18, p. 11-20.

Leissa A. Vibration of plates. Acoustical Society of America, Columbus, Ohio, USA, 1993.

Maluski SPS, Gibbs BM. Application of a finite-element model to low-frequency sound insulation in dwellings. J. of the Acoustical Society of America, 2000, 108, p. 1741-1751.

Metzen HA. Estimation of the reduction in impact sound pressure level of floating floors from the dynamic stiffness of insulation layers, Building Acoustics, 1996, 3, p. 33-53.

Neves e Sousa A. Low frequency impact sound transmission in dwellings. PhD thesis, The University of Liverpool, Liverpol, UK, 2005.

Neves e Sousa A, Gibbs BM. Low frequency impact sound transmission in dwellings through homogenous concrete floors and floating floors. Applied Acoustics, 2011, 72, p. 177-189.

Oniszczuk Z. Free transverse vibrations of an elastically connected rectangular simply supported double-plate complex system, Journal of Sound and Vibration, 2000, 236, p. 595-608;

Oniszczuk Z. Forced transverse vibrations of an elastically complex rectangular simply supported double-plate system, Journal of Sound and Vibration, 2004, 270, p. 997-1011;

Pritz T. Dynamic Young's modulus and loss factor of plastic foams for impact sound isolation, Journal of Sound and Vibration, 1994, 179, p. 315-322;

Pritz T. Dynamic Young's modulus and loss factor of floor covering materials, Applied Acoustics, 1996, 49, p. 179-190;

Schiavi A, Belli AP, Russo F. Estimation of acoustical performance of floating floors from dynamic stiffness of resilient layers, Building Acoustics, 2005, 12, p. 99-113;

Stewart MA, Craik RJM. Impact sound transmission through a floating floor on a concrete slab, Applied Acoustics, 2000, 59, p. 353-372;

Stewart MA, Makenzie RK. A comparison of the predicted dynamic stiffness of resilient layers with calculated values obtained from the measured acceleration response, Building Acoustics, 2000, 7, p. 297-313;

Vér I. Measurement of dynamic stiffness and loss factor of elastic mounts as a function of frequency and static load, Noise Control Engineering, 1974, 3, p. 37-42;

Vieira de Melo GS, Gerges SNY, Gibbs BM. Sound absorption at low frequencies: Modelling a test room. Building Acoustics, 2006, 13, pp. 141-158.

Warburton GB. The vibration of rectangular plates. Proceedings of the Institute of Mechanical Eng, 1954, Ser. A, 168, p. 371-384.